Simulation of Floating Bodies in Waves and Mooring in a 3D Numerical Wave Tank using REEF3D

Tobias Martin* Hans Bihs Arun Kamath Øivind Asgeir Arntsen

Department of Civil and Environmental Engineering, Norwegian University of Science and Technology (NTNU), 7491 Trondheim, Norway

Presented at *4th International Conference in Ocean Engineering.*

Abstract

Mooring systems ensure the safety of structures near the shore like floating breakwaters and aquaculture cages by keeping them in position. Their design has to either provide enough flexibility to allow large displacements or enough strength to withstand the hydrodynamic loads while restraining the structural motion. The accurate determination of the motion of the moored-floating structure and the resulting tension forces in the cables are, therefore, of high significance to produce a safe and economical design. At the same time, the dynamics of the cables can be neglected in the early design process due to their minor contribution to the forces acting on the structure. Hence, an analytical solution for the cables can be found, which provides a fast solution to the problem. The mooring model is implemented in the open-source CFD model REEF3D. The solver has been widely used to study various problems in the field of wave hydrodynamics. It solves the incompressible Reynolds-averaged Navier-Stokes equations for two-phase flows using a finite-difference method and a level set method to model the free surface between water and air. Floating structures are represented by an additional level set function. Its motion is calculated from the Newton and Euler equations in 6DOF and in a non-inertial coordinate system. The fluid-structure interaction is solved explicitly using an immersed boundary method based on the ghost cell method. The application shows the accuracy of the solver and effects of mooring on the motion of a floating structure.

Keywords: CFD; REEF3D; Mooring; Fluid-structure interaction

---

*Corresponding author, tobias.martin@ntnu.no

Postprint, published in 4th International Conference in Ocean Engineering.

1 Introduction

Coupled fluid-structure interaction plays a major role in the fields of coastal and ocean engineering. Most applications require the solution of a two-phase problem as well as an accurate determination of rigid body dynamics. Some examples are floating breakwater, aquaculture cages or ship motion prediction. As a first attempt, fluid-structure interaction problems based on the Navier-Stokes equations have been calculated with Arbitrary Lagrangian-Eulerian methods (Ramaswamy et al., 1986). In this approach, the interface between solid and fluid is tied to the numerical mesh for which reason the mesh needs to be adjusted dynamically. The re-meshing procedure can have a detrimental effect on the numerical accuracy and stability, especially for more arbitrary solid body movements. A way to avoid constant re-meshing is the usage of dynamic overset grids. The method consists of an Eulerian mesh for the fluid and a overset mesh which follows the movement of the solid and overlaps with the base mesh. A stable scheme for establishing the connections between the overset mesh points and the underlying grid points in the overlapping region has to be introduced (see e.g. Carrica et al. (2007)). As an alternative, a direct forcing immersed boundary method was developed for describing the fluid-structure interaction (Yang and Stern, 2012). This immersed boundary method requires just one Eulerian grid and the interaction is incorporated by an additional forcing term in the Navier-Stokes equations. Special attention was also given to the field extension method (Yang and Balaras, 2006), which accounts for solid cells becoming fluid cells and vice versa. With the field extension, unphysical values for the pressure and the velocities are avoided. More recently, Calderer et al. (2014) presented a level set-based two-phase flow solver for the simulation of floating structures. In this work, an extension of the local directional immersed boundary method (Berthelsen and Faltinsen, 2008) using the field extension method is presented. The geometry of the solid is described by a level-set function. Hence, forces and moments can be calculated without explicitly defining the intersections between the surface mesh and the grid of the flow domain. Like other immersed boundary methods, the solid body is immersed into the fluid and re-meshing or overset grids are avoided. The presented results are all obtained with a weakly coupled scheme. In combination with the robust two-phase flow solver REEF3D (Bihs et al., 2016), this results in a stable fluid-structure interaction model. If the motion of the floating structure is large, mooring dynamics can have a significant impact on the response of the structure. The general solution for the dynamics of mooring systems has to be found numerically due to the underlying non-linear system of equations. Several discretization methods have been developed, like the finite differences (Huang, 1994) and finite element based methods (Aamo and Fossen, 2001) or the lumped mass method (Hall and Goupee, 2015). A general overview of the methods can be found in Davidson and Ringwood (2017). For structures with small responses in mild environmental conditions, a quasi-static mooring model is suitable. By neglecting the dynamic effects of the mooring system, dependencies of mass, damping and fluid acceleration on the system are omitted. The mooring line shape and tension can then be found analytically as shown by Faltinsen (1990). It has the advantage of computational efficiency and simplicity of implementation. Therefore, the analytical approach is taken into account in this paper as a starting point for more advanced models in the further research. In section 2 the CFD model REEF3D is shortly described. Afterwards, details about the implemented 6DOF algorithm and mooring model are given in section 2.1 and 2.2. The application of the solver is presented in section 3. Final remarks and prospects for further developments can be found in section 4.

2 Numerical Model

The basic equations of the numerical model arise from the conservation law of mass and momentum for incompressible fluids. Using tensor notation, the resulting equations read for a whole-domain formulation

$$\frac{\partial u_i}{\partial x_i} = 0, \tag{1}$$

$$\frac{\partial u_i}{\partial t} + u_j \frac{\partial u_i}{\partial x_j} = -\frac{1}{\rho}\frac{\partial p}{\partial x_i} + \frac{\partial}{\partial x_j}\left(\nu \cdot \left(\frac{\partial u_i}{\partial x_j} + \frac{\partial u_j}{\partial x_i}\right)\right) + g_i, \tag{2}$$

with u_i the velocity components, ρ the fluid density, p the pressure, ν the kinematic viscosity and $\vec{g}$ the gravity acceleration vector. Here, the Reynolds-averaged Navier-Stokes (RANS) equations are solved by replacing the fluid properties with time-averaged values and add turbulent viscosity to ν. The additional viscosity is calculated with a modified k-ω model as given in Bihs et al. (2016).

The spatial domain is discretised by a finite difference method (FDM) on a Cartesian grid. System (1), (2) is solved on a staggered grid to avoid decoupling of pressure and velocity. Convection terms are evaluated in a non-conservative form because the violation of the mass conservation during an explicit solution procedure might cause numerical instabilities in a conservative formulation (Sussman et al., 1994). For this purpose, the fifth-order accurate weighted essentially non-oscillatory (WENO) scheme of Jiang and Shu (1996) adapted to non-conservative terms by Zhang and Jackson (2009) is applied. The discretised system is solved using Chorin's projection method for incompressible flows (Chorin, 1968). The pressure is calculated from a Poisson equation and applying the fully parallelized BiCGStab algorithm (van der Vorst, 1992). For progressing in time, the third-order accurate Total Variation Diminishing (TVD) RungeKutta scheme (Shu and Osher, 1988) is employed. Adaptive time stepping controls the time stepping according to the required CFL condition.

The location of the free water surface is represented implicitly by the zero level set of a smooth signed distance function $\Phi(\vec{x}, t)$ which is defined as the closest distance to the interface (Osher and Sethian, 1988). Its motion can be described by the advection equation

$$\frac{\partial \Phi}{\partial t} + u_j \frac{\partial \Phi}{\partial x_j} = 0. \tag{3}$$

The convection term in (3) is discretised by the fifth-order accurate Hamilton-Jacobi WENO method of Jiang and Peng (2000). In order to conserve the signed distance property, the level set function is reinitialized after each time step. Here, the PDE-based reinitialization equation of Sussman et al. (1994) is taken into account. The material properties of the two phases are finally determined for the whole domain in accordance to the continuum surface force model of Brackbill et al. (1992) (see Bihs et al. (2016) for details).

2.1 6DOF Algorithm

The geometry of the rigid body is described by a primitive triangular surface mesh neglecting connectivity. For this purpose, the intersections of the surface mesh with the underlying Cartesian grid are determined with the ray-tracing algorithm of Yang and Stern (2014). It efficiently provides inside-outside information and, for each grid point, the shortest distance

along the coordinate axis to the body describing triangles. Afterwards, the mentioned reinitialization algorithm of Peng et al. (1999) is applied to obtain signed distance properties for a level set function in the vicinity of the solid body. This has the advantage that the intersections of the surface mesh with the underlying grid do not have to be calculated explicitly. The obtained level set function can be used for calculating the six force and moment components of the fluid on the body as given by Bihs and Kamath (2017).

Any point relating to a rigid body can be described by the location the centre of gravity and orientation of the body in the inertial coordinate system. Here, the orientation is described by Euler angles which results in the position vector

$$\vec{x} = \left(x_1, x_2, x_3, x_4, x_5, x_6\right)^{\mathcal{T}}, \tag{4}$$

where the first components are the coordinates of the centre of gravity and the last three components are the Euler angles ϕ, θ and ψ. The calculation of the motion of a body in the inertial system would include several time derivatives of moments which can be avoided by applying a coordinate transformation to the Euler equations. The rotation components in the principal coordinate system of the body reads then

$$\vec{\xi} = \left(\xi_1, \xi_2, \xi_3\right)^{\mathcal{T}}. \tag{5}$$

In this paper, it is assumed that the principal axes of the body are known. Thus, the inertia tensor reduces to the three principal moments of inertia which yields

$$\vec{I} = \begin{bmatrix} I_x & 0 & 0 \\ 0 & I_y & 0 \\ 0 & 0 & I_z \end{bmatrix} = \begin{bmatrix} mr_x^2 & 0 & 0 \\ 0 & mr_y^2 & 0 \\ 0 & 0 & mr_z^2 \end{bmatrix}, \tag{6}$$

with m the mass of the body and r_x, r_y and r_z the distances of a point from the centre of gravity along the $x-$,$y-$ and $z-$direction. Since the fluid flow is calculated in the inertial system, the acting moments in this system $\vec{M}_{\vec{x}}$ have to be transformed to the non-inertial system by applying the transformation (Fossen, 1994)

$$\vec{M}_{\vec{\xi}} = \left(M_{1,\vec{\xi}}, M_{2,\vec{\xi}}, M_{3,\vec{\xi}}\right)^{\mathcal{T}} = \vec{J}_1^{-1} \cdot \vec{M}_{\vec{x}}, \tag{7}$$

with $\vec{M}_{\vec{\xi}}$ the moments in the system of the body and $\vec{J}_1^{-1}$ the rotation matrix (s stands for sin and c for cos)

$$\vec{J}_1 = \begin{bmatrix} cx_6cx_5 & -sx_6cx_4 + cx_6sx_5sx_4 & sx_6sx_4 + cx_6cx_4sx_5 \\ sx_6cx_5 & cx_6cx_4 + sx_4sx_5sx_6 & -cx_6sx_4 + sx_5sx_6cx_4 \\ -sx_5 & cx_5sx_4 & cx_5cx_4 \end{bmatrix}. \tag{8}$$

Hence, the dynamics of the rigid body can described by the three equations of translational motion

$$\begin{pmatrix} \ddot{x}_1 \\ \ddot{x}_2 \\ \ddot{x}_3 \end{pmatrix} = \frac{1}{m} \cdot \begin{pmatrix} F_{x_1,\vec{x}} \\ F_{x_2,\vec{x}} \\ F_{x_3,\vec{x}} \end{pmatrix}, \tag{9}$$

where $F_{\vec{x}}$ are the acting forces in the inertial system, and the three Euler equations in the non-inertial system (Fossen, 1994)

$$\begin{aligned} I_x\ddot{\xi_1} + \dot{\xi_2}\dot{\xi_3} \cdot (I_z - I_y) &= M_{1,\vec{\xi}}, \\ I_y\ddot{\xi_2} + \dot{\xi_1}\dot{\xi_3} \cdot (I_x - I_z) &= M_{2,\vec{\xi}}, \\ I_z\ddot{\xi_3} + \dot{\xi_1}\dot{\xi_2} \cdot (I_y - I_x) &= M_{3,\vec{\xi}}. \end{aligned} \tag{10}$$

The position of the body can be calculated analytically by integrating (9) twice. System (10) is solved explicitly with the second-order accurate Adams-Bashforth scheme which reads for a generic variable in the new time step $q^{(n+1)}$

$$\dot{q}^{(n+1)} = \dot{q}^{(n)} + \frac{\Delta t}{2} \cdot \left(3\ddot{q}^{(n+1)} - \ddot{q}^{(n)}\right), \tag{11}$$

$$q^{(n+1)} = q^{(n)} + \frac{\Delta t}{2} \cdot \left(3\dot{q}^{(n+1)} - \dot{q}^{(n)}\right). \tag{12}$$

The Euler angles in the body system cannot be calculated from the body angular velocities due to missing physical interpretation (Fossen, 1994). Instead, the angular velocities are transformed back using the rotation matrix (s stands for sin, c for cos and t for tan)

$$\vec{J_2} = \begin{bmatrix} 1 & sx_4tx_5 & cx_4 + cx_6tx_5 \\ 0 & cx_4 & -sx_4 \\ 0 & sx_4/cx_5 & cx_4/cx_5 \end{bmatrix}. \tag{13}$$

Afterwards, the necessary Euler angles are calculated from (12) in the inertial frame. It might be noticed that (13) has a singularity at $x_5 = \pm\frac{\pi}{2}$. In practice, this angle does not occur for typical floating structures in ocean engineering.

In this paper, the fluid-structure coupling is arranged in a weak form without sub-iterations. First, acting forces are calculated from the fluid, and the body position is determined as described above. Afterwards, the fluid properties are updated to the new time level using the ghost cell immersed boundary method (Berthelsen and Faltinsen, 2008) for incorporating the boundary conditions of the solid. For both the velocities and the pressure, these conditions are calculated from the motion of the body with respect to its centre of gravity (Bihs and Kamath, 2017). Even though the weak coupling has been reported to lead to numerical stability problems for complex cases (e.g., Carrica et al. (2007) or Calderer et al. (2014)), the current implementation shows good numerical stability throughout the range of application. However, pressure oscillations can occur in the vicinity of the solid body because of solid cells turning into fluid cells. The fresh fluid cells lack physical information about velocities from previous time steps. It is solved by implementing the field extension method of Yang and Balaras (2006); Udaykumar et al. (2001) adapted to the ghost cell immersed boundary method.

2.2 Mooring Model

The mooring systems considered in this paper consist of a number of cables which are attached to the floating structure at arbitrary points. Their lower ends are anchored at the sea bed. In order to avoid high vertical forces on the anchor, a part of the cable lies on the bottom, and

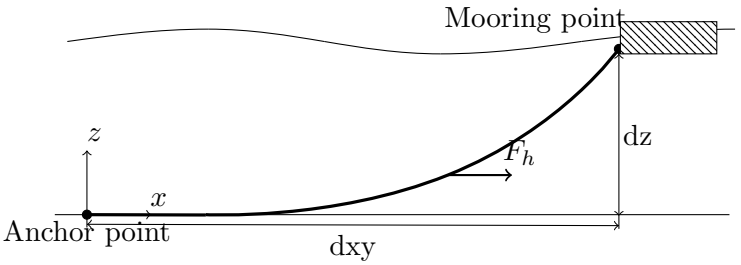

Figure 1: Definition of a mooring line in two dimensions.

damps the vertical motion of the structure. An illustration of this configuration can be seen in figure 1. The general equations describing the unsteady motion of a cable are non-linear and have to be solved numerically. For practical purposes, an analytical solution can be found if static conditions and no current forces are assumed. Following the derivation of Faltinsen (1990), a catenary equation, describing the shape of a line, arises as

$$z(x,y) = \frac{F_h}{w} \cdot \left(\cosh\left(\frac{w}{F_h} \cdot \sqrt{x^2+y^2} \right) \right), \tag{14}$$

with F_h the horizontal force, which is constant along the cable, and w the weight per unit length of the cable in water. The tension forces F_t are calculated as

$$F_t(z) = F_h + wdz + (z - dz) \cdot (w + \rho g A), \tag{15}$$

where g is the acceleration due to gravity and A is the cross-section area of the cable. The area is assumed to be constant, i.e., elasticity of the material is neglected. In the current algorithm, the effect of the mooring lines on the dynamics of the structure is taken into account explicitly in a weakly coupled manner. For this purpose, the forces of each cable acting on the structure have to be calculated from the known distance dxy from the time-invariant anchor point to the current position of the mooring point. The corresponding equation is written as (Faltinsen, 1990)

$$dxy = \sqrt{dx^2+dy^2} = l - dz \cdot \sqrt{1 + 2 \cdot \frac{F_h}{wdz}} + \frac{F_h}{w} \cosh^{-1}\left(1 + \frac{wdz}{F_h}\right), \tag{16}$$

which provides a function transcendental in F_h. A solution can be determined using the Newton-Raphson algorithm

$$F_h^{(k+1)} = F_h^{(k)} - \frac{f(F_h^{(k)})}{f'(F_h^{(k)})}, \quad k = 1, 2, ... \tag{17}$$

Once, a converged solution for F_h has been found, the forces at each mooring point X, Y, Z result from

$$X = F_h \cos\left(\tan^{-1}\left(\frac{dy}{dx} \right) \right), \tag{18}$$

$$Y = F_h \sin\left(\tan^{-1}\left(\frac{dy}{dx} \right) \right), \tag{19}$$

$$Z = F_h dz \cdot \sqrt{1 + \frac{2F_h}{wdz}}, \tag{20}$$

and moments by multiplication with the appropriate distances to the centre of gravity of the body.

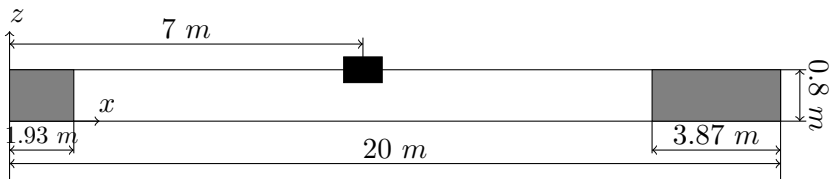

Figure 2: Setup for the test case of a 2D barge in waves.

3 Results for a 2D barge in waves

The capability of the presented 6DOF algorithm is presented for a rigid floating barge in two dimensions under the effect of waves with and without mooring. The results are compared to the experimental data of Ren et al. (2015). The laboratory experiment was performed in a wave flume of $20m$ length, $0.8m$ height and $0.44m$ width, which is modelled with the numerical wave tank of REEF3D (Bihs et al., 2016). The barge is $0.30m$ long and $0.2m$ high. Since the gap between body and flume walls is small, the case can be considered as 2D, with surge, heave and pitch motion. The initial position of the barge is defined by its centroid at $(x, z) = (7.0m, 0.4m)$. Its density is $500kg/m^3$. The water depth in the tank is $d = 0.4m$. The incoming waves are regular and have a height of $0.04m$, a period $T = 1.2s$ and wavelength of $1.936m$. In the calculations these are modelled using a second-order Stokes wave theory. A numerical beach is applied in order to avoid wave reflections at the outlet. For the discretisation, a cell size of $0.005m$ is chosen which equals $640,000$ cells.

3.1 Free-Floating Condition

The results from the free-floating simulation are compared with the experiment for the period between $t/T = 6.36s$ and $t/T = 12s$. The wave elevation shown in figure 3a shows a good agreement with the experimental data, which confirms the chosen wave theory for modelling the waves. In accordance to the quality of the incoming waves, the distribution of the pitch motion predicts accurate results for most part of the simulation. Small undershoots are given which correspond to under-predicted wave troughs at $t/T = 9.3$ and $t/T = 11.3$ (see figure 3b). Also, underresolved damping effects from vortex detaching at the immersed edges might influence the accuracy of the pitch motion. The frequency of the heave motion follows the frequency of the experimental data accurately. However, the amplitudes of this motion are 10% smaller in the simulations. This might be caused by the coupled physics of heave and pitch motion. In contrast, the surge motion is predicted much better, showing a good accordance of the drift with the experiments. This drift is mainly caused by inertia effects driven by the wave motion which is accurately predicted here.

3.2 Moored Condition

The effect of mooring and capability of the presented mooring model is shown for the 2D barge in waves. For this purpose, two mooring lines are fixed to the body at $z = 0.4m$. The

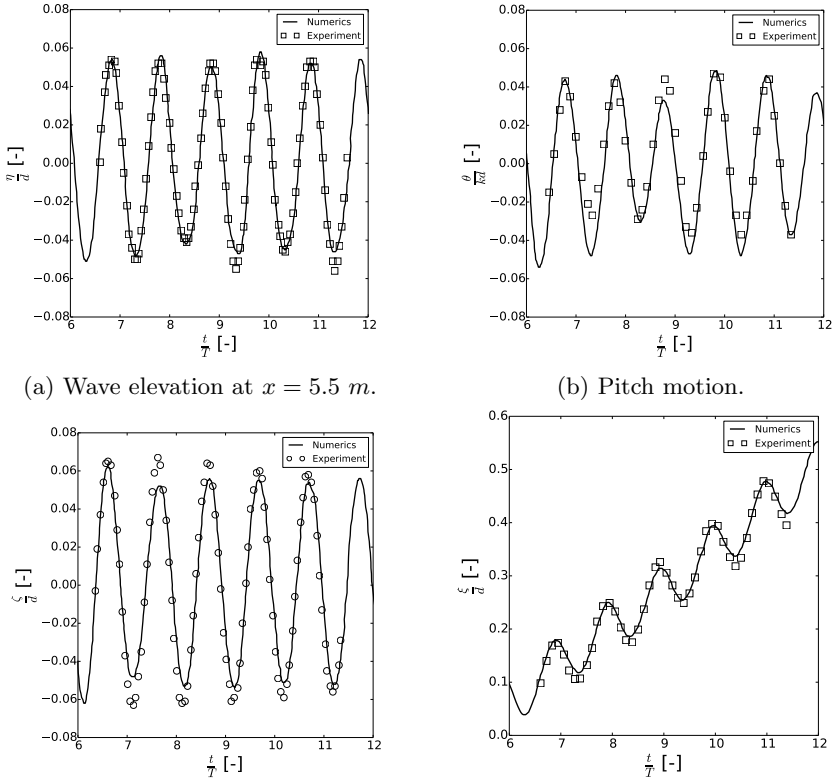

(a) Wave elevation at $x = 5.5\ m$.

(b) Pitch motion.

(c) Heave motion.

(d) Surge motion.

Figure 3: Numerical results of the two-dimensional barge in comparison to the experiment data.

cables are $1.6m$ long, $0.01m$ thick and have a weight per unit length of $w = 4kg/m$ in water. A comparison to the motion from above is ensured by increasing the weight of the free-floating body resulting in the same draft as initial condition. As results, the heave and surge motions over time are shown in figure 5. The vertical motion of the structure is significantly damped by installing the mooring system. Further, surging is prevented almost completely.

4 Conclusion

This paper gives an overview of the implementation of a weakly-coupled 6DOF algorithm in the open-source CFD code REEF3D. The floating body is represented by the combination of a surface mesh, a level set function, and the ghost cell immersed boundary method. This results in a method that does not require re-meshing or overset grids. In addition, a simple mooring model is presented which provides analytical solutions for the shape and forces of mooring systems. The application confirms the accuracy of REEF3D in modelling fluid-structure interactions. The mooring model is able to provide the damping effects on the motion of floating bodies. However, for more advanced mooring applications, like tension-leg platforms and extreme weather situations, a dynamic model is preferable.

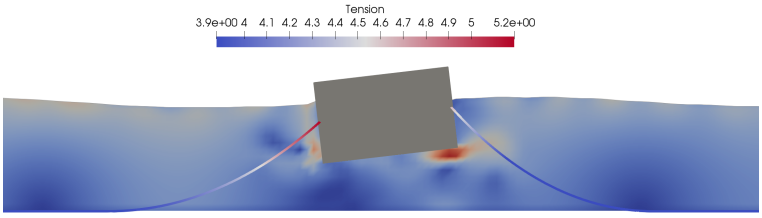

Figure 4: Tension force distribution in the mooring cables during a wave trough situation.

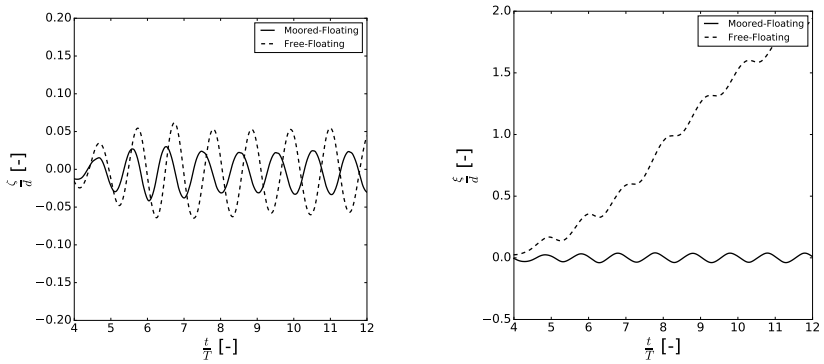

(a) Heave Motion. (b) Surge motion.

Figure 5: Numerical results of the free-floating and moored-floating two-dimensional barge.

Acknowledgements

The calculations were supported in part with computational resources at the Norwegian University of Science and Technology (NTNU) provided by NOTUR project (No. NN2620K), http://www.notur.no.

References

Aamo, O. and Fossen, T. (2001). Finite Element Modelling of Moored Vessels. *Mathematical and Computer Modelling of Dynamical Systems*, **Volume 7(1)**, 47–75.

Berthelsen, P. and Faltinsen, O. (2008). A local directional ghost cell approach for incompressible viscous flow problems with irregular boundaries. *Journal of Computational Physics*, **Volume 227**, 4354–4397.

Bihs, H. and Kamath, A. (2017). A combined level set/ghost cell immersed boundary representation for floating body simulations. *Int. J. Numer. Meth. Fluids*, **Volume 83**, 905–916.

Bihs, H., Kamath, A., Chella, M.A., Aggarwal, A. and Arntsen, Ø.A. (2016). A new level set numerical wave tank with improved density interpolation for complex wave hydrodynamics. *Computers & Fluids*, **Volume 140**, 191–208.

Brackbill, J., Kothe, D. and Zemach, C. (1992). A Continuum Method for Modeling Surface Tension. *Journal of Computational Physics*, **Volume 100(2)**, 335–354.

Calderer, A., Kang, S. and Sotiropoulos, F. (2014). Level set immersed boundary method for coupled simulation of air/water interaction with complex floating structures. *Journal of Computational Physics*, **Volume 277**, 201–227.

Carrica, P., Noack, R. and Stern, F. (2007). Ship motions using single-phase level set with dynamic overset grid. *Computers & Fluids*, **Volume 36**, 1415–1433.

Chorin, A. (1968). Numerical solution of the Navier-Stokes equations. *Mathematics of Computation*, **Volume 22**, 745–762.

Davidson, J. and Ringwood, J. (2017). Mathematical modelling of mooring systems for wave energy converters-A review. *Energies*, **Volume 10**, 666.

Faltinsen, O. (1990). *Sea Loads on Ships and Offshore Structures*. Cambridge University Press, Cambridge.

Fossen, T. (1994). *Guidance and Control of Ocean Vehicles*. John Wiley & Sons: Chichester, England.

Hall, M. and Goupee, A. (2015). Validation of a lumped-mass mooring line model with DeepCwind semisubmersible model test data. *Ocean Engineering*, **Volume 104**, 590–603.

Huang, S. (1994). Dynamic analysis of three-dimensional marine cables. *Ocean Engineering*, **Volume 21**, 587–605.

Jiang, G. and Peng, D. (2000). Weighted ENO schemes for Hamilton Jacobi equations. *SIAM Journal of Scientific Computing*, **Volume 21**, 2126–2143.

Jiang, G. and Shu, C. (1996). Efficient implementation of weighted ENO schemes. *Journal of Computational Physics*, **Volume 126(1)**, 202–228.

Osher, S. and Sethian, J. (1988). Fronts propagating with curvature-dependent speed: Algorithms based on Hamilton-Jacobi formulations. *Journal of Computational Physics*, **Volume 79**, 12–49.

Peng, D., Merriman, B., Osher, S., Zhao, H. and Kang, M. (1999). A PDE-based fast local level set method. *Journal of Computational Physics*, **Volume 155**, 410–438.

Ramaswamy, B., Kawahara, M. and T.Nakayama (1986). Lagrangian finite element method for the analysis of two-dimensional sloshing problems. *International Journal for Numerical Methods in Fluids*, **Volume 6**, 659–670.

Ren, B., He, M., Dong, P. and Wen, H. (2015). Nonlinear simulations of wave-induced motions of a freely floating body using WCSPH method. *Applied Ocean Research*, **Volume 50**, 1–12.

Shu, C. and Osher, S. (1988). Efficient implementation of essentially non-oscillatory shock-capturing schemes. *Journal of Computational Physics*, **Volume 77(2)**, 439–471.

Sussman, M., Smereka, P. and Osher, S. (1994). A level set approach for computing solutions to incompressible two-phase flow. *Journal of Computational Physics*, **Volume 114**, 146–159.

Udaykumar, H., Mittal, R., Rampunggoon, P. and Khanna, A. (2001). A sharp interface cartesian grid method for simulating flows with complex moving boundaries. *Journal of Computational Physics*, **Volume 174**, 174–345.

van der Vorst, H. (1992). BiCGStab: A fast and smoothly converging variant of Bi-CG for the solution of nonsymmetric linear systems. *SIAM Journal of Scientific Computing*, **Volume 13**, 631–644.

Yang, J. and Balaras, E. (2006). An embedded-boundary formulation for large-eddy simulation of turbulent flows interacting with moving boundaries. *Journal of Computational Physics*, **Volume 215**, 12–40.

Yang, J. and Stern, F. (2012). A simple and efficient direct forcing immersed boundary framework for fluid?structure interactions. *Journal of Computational Physics*, **Volume 231**, 5029?5061.

Yang, J. and Stern, F. (2014). Robust and efficient setup procedure for complex triangulations in immersed boundary simulations. *Journal of Fluids Engineering*, **Volume 135(10)**, 1101107.1?101107.11.

Zhang, J. and Jackson, T.L. (2009). A high-order incompressible flow solver with WENO. *Journal of Computational Physics*, **Volume 228**, 146–159.